Rapid removal of fluoride from water using core@shell and @shell nanoparticles of SiO_2@ZrO_2 and @ZrO_2. Investigation of the mechanisms involved and impact of elemental leaching

Iván Maisuls[b], Yolanda Castro[c], Alicia Durán[c], Dominic Larivière[d], Pablo M. Arnal[,a,b]*

a: Facultad de Ciencias Exactas, Universidad Nacional de La Plata, 1 y 115, 1900, La Plata, Argentina

b: CETMIC (Centro de Tecnología de Recursos Minerales y Cerámica) - CONICET, Centenario y 506, CC 49 (B1897ZCA), M.B. Gonnet, Prov. Buenos Aires, Argentina

c: Instituto de Cerámica y Vidrio (CSIC), Kelsen, 5 28049, Madrid, Spain

d: Département de chimie, Faculté des sciences et de génie, Université Laval, 1045, avenue de la Médecine, Québec, Qc, Canada, G1V 0A6

* Corresponding author:

E-mail: arnal@quimica.unlp.edu.ar

Key Words: zirconium oxide; core@shell; @shell; fluoride removal from water; silica; leaching; fluorocomplex; RSM.

Abstract

Fluoride is a natural contaminant of water that endangers many people worldwide when present in concentrations higher than 2 ppm. Here, fluoride removal by four different nanostructured colloidal particles ($SiO_2@ZrO_2^{nc}$, $SiO_2@ZrO_2^{c}$, $@ZrO_2^{nc}$, and $@ZrO_2^{c}$) was measured in batch systems within a period of 24 h. Surprisingly, these materials removed fluoride from the water solutions and reached equilibrium in less than 10 minutes. The combination of high specific surface and fast fluoride removal placed these materials among the top materials currently known in fluoride removal. Also, the impact of element leaching was measured and quantified. The influence of time, pH, and fluoride concentration on leaching of Zr and Si was evaluated with a response surface methodology. Leaching of Zr and Si continued for several hours and depended on first-order, quadratic and cross-product coefficients. Previous studies of fluoride removal with zirconium oxide often assumed that a decrease in fluoride concentration in the solution indicated that fluoride was bound to the surface of the oxide. Zirconium oxide's solubility in water is low, but not zero. Hence, Zr might have formed soluble fluorocomplexes. This is the first report of fluoride removal with zirconium oxide that studied the leaching of the solid to exclude the formation of soluble fluorocomplexes.

Highlights

- $SiO_2@ZrO_2$ and $@ZrO_2$ removed fluoride from water in less than 10 min.
- Materials can be easlily removed from the water solution.
- Si and Zr leached from the solid for hours.
- Formation of fluorocomplexes with Si or Zr is unlikely.
- Leaching from solid material may trigger secondary processes that interfere with the removal process.

Introduction

Fluoride, a natural contaminant of water worldwide [1], [2], is toxic for humans in concentrations higher than 2 parts per million (ppm) [3]. Therefore, several groups from the scientific community focused their interest on fluoride removal from water.

Zirconium-based materials emerged as promising candidates to remove fluoride from water [4]–[7]. The strong affinity between zirconium and fluoride is a critical driving force behind these materials' potentiality in fluoride removal. Synthesis protocols for zirconium-based materials with high specific-surface-areas (>100 $m^2.g^{-1}$) are available in the scientific literature [8]–[10].

When researching fluoride removal, scientists indirectly determined the amount of fluoride attached to the solid. These indirect measurements consider that fluoride drops its concentration in solution because it binds to the solid's surface. Some scientists considered this assumption valid for a range of pH values from 3 to 10. For example, Dou *et al*. [11] reported that hydrous zirconium oxides reached fluoride removal capacities of 120 mg/g at pH = 3. At the same pH value, Liao and Shi [12] reported that zirconium impregnated collagen fibers reached fluoride removal capacities of 37 mg/g.

Assuming that fluoride can only change its concentration because it binds to the solid may understate what happens in the system. First, zirconium chemically reacts with fluoride forming soluble fluorocomplexes. Second, zirconium's solubility skyrockets when pH turns acid in the presence of fluoride (hydrofluoric acid). Both facts suggest that fluoride may chemically react with the zirconium-based material and form soluble fluorocomplexes. Hence, fluoride may change its concentration in solution because of other chemical reactions that consume fluoride.

This work aims to preliminary assess the assumption that supports the indirect method of fluoride quantification in water. This work hypothesizes that silicon and zirconium would leach from the solid during batch experiments, but soluble fluorocomplexes would not significantly form. We will test our hypothesis with four different types of nanostructured particles of zirconium oxide in batch systems.

2 Materials and Methods

2.1 Synthesis of Nanostructured Colloidal Particles

A set of four different types of spherical colloidal particles was prepared following a procedure described elsewhere [8], [10]: **$SiO_2@ZrO_2^{nc}$**, **$SiO_2@ZrO_2^{c}$**, **$@ZrO_2^{nc}$**, and **$@ZrO_2^{c}$** (see Figure 1 for a more comprehensive description of synthesis pathway and particle's structure). In the first step of the synthesis, monodisperse colloidal silica particles were formed. In the second step, these silica spheres were individually covered with a nanometer-thick, homogeneous layer forming a core@shell architecture where both core and shell were non-crystalline (symbolized **$SiO_2@ZrO_2^{nc}$**). From these $SiO_2@ZrO_2^{nc}$ particles, two different pathways followed. First, the silica core was selectively dissolved with aqueous NaOH 1N to form hollow, non-crystalline zirconium oxide spheres (**$@ZrO_2^{nc}$**). Second, the shell crystallized upon been subjected to a thermal treatment but not the silica core forming a new type of particles (**$SiO_2@ZrO_2^{c}$**). In the last step of the synthesis, $SiO_2@ZrO_2^{c}$ particles treated with aqueous NaOH 1N convert into hollow spheres of crystalline zirconium oxide (**$@ZrO_2^{c}$**).

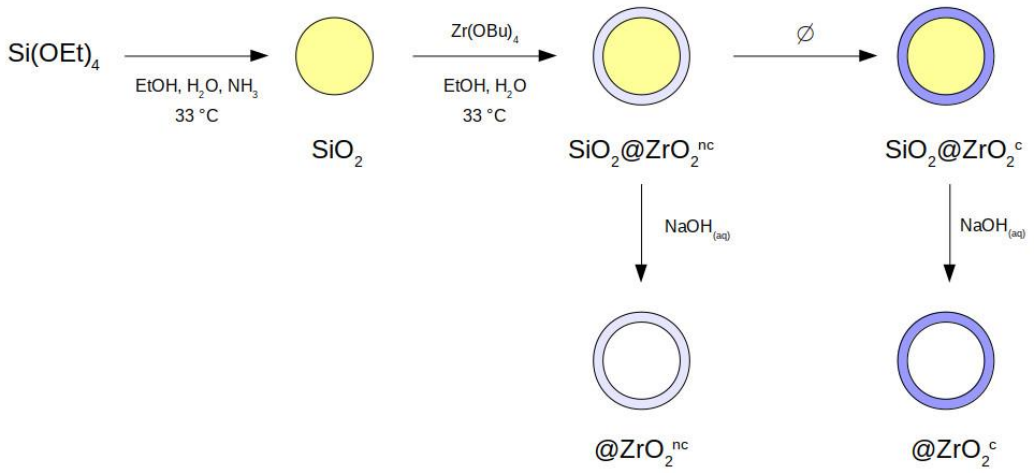

Figure 1. Flow-chart of the synthesis of the four types of nanostructured colloidal particles used in this study: two types of core@shell and two types of @shell (*i.e.*, hollow) spheres. Silica is non-crystalline. The superscripts indicate whether the zirconia shell is non-crystalline (nc) or crystalline (c). The four types of particles are the following: **$SiO_2@ZrO_2^{nc}$**, **$SiO_2@ZrO_2^{c}$**, **$@ZrO_2^{nc}$**, and **$@ZrO_2^{c}$**.

2.2 Particle Characterization

Field-Emission Scanning Electron Microscopy

Field-Emission Scanning Electron Microscopy (Hitachi-H7100, Japan) was used to analyze the morphology (shape, size, and size distribution) of nanostructured core@shell and @shell particles.

X-ray diffraction

X-ray diffraction (Diffractometer Philips PW 3710, Goniometer Philips 3020, Cu K_α radiation, 40 kV, 35 mA, range 20-40º 2θ, step 4 s) was used to identify crystalline phases (or their absence) in all four types of particles. Based on Powder Diffraction Data Base version PDF-2 from International Centre for Diffraction Data (ICDD), we assigned reflexes in diffractograms.

Light scattering

The particle sizes were measured using a laser diffraction equipment Mastersizer S, Malvern He-Ne LASER, λ=632.8 nm). The different core@shell or @shell particles were dispersed in water and measured.

2.3 Fluoride Removal in Batch Experiments

The ability of all four types of nanostructured colloidal particles to remove fluoride from the water was tested in batch mode. 25.0 mL of NaF solution (10.00 ppm) was poured into a polypropylene flask (25 mL, screw cap) containing 30 mg of solid. Closed flasks were shaken mechanically for 0 to 1500 min. Subsequently, the solid was separated from the solution by centrifugation (6 min; 5000 rpm). Then, fluoride concentration was determined spectrophotometrically following a previously reported procedure [13]. Briefly, 5 g of the solution recovered from the batch system was mixed with 45 g of MQ water, and 10.67 g of SPANDS-Zr solution into a polypropylene flask (150 mL, screw cap). Blank measurements were obtained with a solution of SPANDS in the HCl solution. The UV-Vis spectrometer (HP 8453, tungsten lamp) was calibrated using a standard solution of fluoride (1.000 ppm, Chem-Lab). Absorbance was measured at λ = 570 nm.

2.4 Leaching Test in Batch Mode (Design of Experiment)

A response surface methodology (RSM) [14] using a face-centered central composite experimental design was used to study the leaching process of elements from the nanostructure colloidal particles during the removal of fluoride. This experimental design was performed by measuring dissolved concentrations of Na, Si, and Zr, which compose the solid particles used in this study [8]. The influence on the leaching process of three factors (time, pH, and initial F^- concentration ($[F^-]_i$) at two levels each was investigated in the proposed experimental design. The assessment ranges for those factors were: time (0, 48 h), pH (4.5, 8.5), and initial fluoride concentration (2, 10 ppm). To estimate the experimental error, the design included centre points analysis in triplicate. Table 1 shows the codification used for this experimental design.

Table 1. Codification used in the experimental design using a face-centered central composite experimental design with center points analysis.

Code	Time (h)	pH	$[F^-]_i$ (ppm)
1	0	4,5	2
2	0	4,5	10
3	0	8,5	2
4	0	8,5	10
5	0	6,5	6
6	24	4,5	6
7	24	8,5	6
8	24	6,5	2
9	24	6,5	10
10	24	6,5	6
11	24	6,5	6
12	24	6,5	6
13	48	4,5	2
14	48	4,5	10
15	48	4,5	2
16	48	8,5	10
17	48	8,5	6

Solutions for batch systems used in leaching experiments were prepared with the following chemicals: High-purity water with a resistivity of 18.2 MΩ.cm provided by a Milli-Q water purification system (Millipore, Etobicoke, ON, Canada); KOH (Fisher Scientific,

Ottawa, ON, Canada) and HNO_3 (Anachemia Chemical, Montreal, QC, Canada) to adjust pH; KNO_3 (Anachemia Chemical, Montreal, QC, Canada) to adjust ionic strength; and KF (J.T.Baker Chemical Co., Phillipsburg, NJ, USA) to set the fluoride concentration.

Moreover, batch mode samples were prepared by mixing 0.1 mL of an aqueous suspension of the solid particles (ca. 1 ppm) with 0.1 mL of KNO_3 0.1 M and 4.8 mL of an aqueous solution with the proper pH and fluoride ion concentration. Upon mixing the constituents, some samples were immediately centrifuged (t = 0) or shaken for a specified period of time (t = 24 or 48h) prior to centrifugation (4700 rpm, 30 minutes).

After centrifugation, dissolved concentrations of Na, Zr, and Si were quantified using an ICP–MS/MS (Agilent 8800 ICP-MS). Using this instrument, detection limits (LOD) based on Equation (1), where σ and m represent the standard deviation of blanks triplicates and the instrumental sensitivity for the analyte of interest, respectively. LOD were calculated to be 3.8, 73.6, and 0.3 μg L^{-1} for Na, Si, and Zr, respectively. By computing the measurements using the statistical software JMP 10 (SAS Institute Inc., Cary, NC, USA), we obtained several indicators such as least squares method, analysis of variance, factors and quadratic graphical analysis as well as the response profiles. Statistical significance for an alpha value of 0.05 was selected.

$$LOD = \frac{3\sigma}{m} \quad (1)$$

2.5 Estimating the Fluoride Concentration Required to Form Hexafluorocomplexes

Both Zr and Si can form hexafluorocomplexes that are soluble in water. Therefore, fluoride ions may chemically attack particles during the batch mode experiment by entering the coordination sphere of either Zr or Si and forming soluble fluorocomplexes. Such a process is unwelcomed as the aim of the removal process is to bind fluoride to the solid, nanostructured particles.

Equation (2), that relates the amount of fluoride removed from the solution with the amount of Zr (or Si) dissolved, can help understand whether such a process occurs. Derived from stoichiometry (see SI), the proposed formula enables to determine the percent of fluoride removed from the solution that could be explained by the formation of soluble hexafluorocomplexes with Zr (or Si):

$$Fluoride\% = \frac{600 \cdot [Zr] \cdot AW_F}{[F^-] \cdot AW_{Zr}} \quad (2)$$

Where [Zr] represents the Zr concentration measured in the aqueous phase (in ppm), [F^-] the fluoride concentration (in ppm), AW_F the atomic weight of fluoride, and AW_{Zr}, the atomic weight of Zr. To derive a similar formula that would estimate the percent of fluoride involved in the formation of hexafluorocomplexes of silicon, [Zr] and AW_{Zr} should be replaced by [Si] and AW_{Si}, respectively.

2.6 Changes in Colloidal Particles with Fourier Transformed Infrared Spectroscopy

Before and after experiments performed in batch mode, chemical groups in nanostructured colloidal particles were analyzed by Fourier transformed infrared spectroscopy. Spectra were recorded in transmission mode in the range of 4000 – 400 cm^{-1} with a resolution of 2 cm^{-1} using a Perkin Elmer FTIR Spectrum 100 equipment. Pellets were prepared by homogeneously mixing 1 mg of the material with 300 mg of KBr. The deconvolution of spectra was performed using Gaussian curves by Origin program.

Results

Synthesis of core@shell and @shell particles

All four types of particles ($SiO_2@ZrO_2^{nc}$, $SiO_2@ZrO_2^{c}$, $@ZrO_2^{nc,}$ and $@ZrO_2^{c}$) were successfully synthesized. X-ray diffraction confirmed the absence of crystalline peaks in $SiO_2@ZrO_2^{nc}$ and $@ZrO_2^{nc}$, but showed sharp reflexes associated with a crystalline tetragonal phase of ZrO_2 in $SiO_2@ZrO_2^{c}$ and $@ZrO_2^{c}$ (01-079-1767) (diffractograms not shown). Field Emission Scanning Electron Microscopy images of all four types of particles highlighted the formation of spherical monodisperse particles (Figure 2). Additionally, light scattering experiments demonstrated that all four types of nanostructured particles tend to cluster when dispersed in an aqueous solution. These clusters had a mean diameter ranging from 2 to 4 μm depending on the nature of the nanostructured particles. Besides, a small portion of $@ZrO_2^{c}$ particles aggregated to form more massive clusters with an average size of 15 and 20 μm (Figure S1).

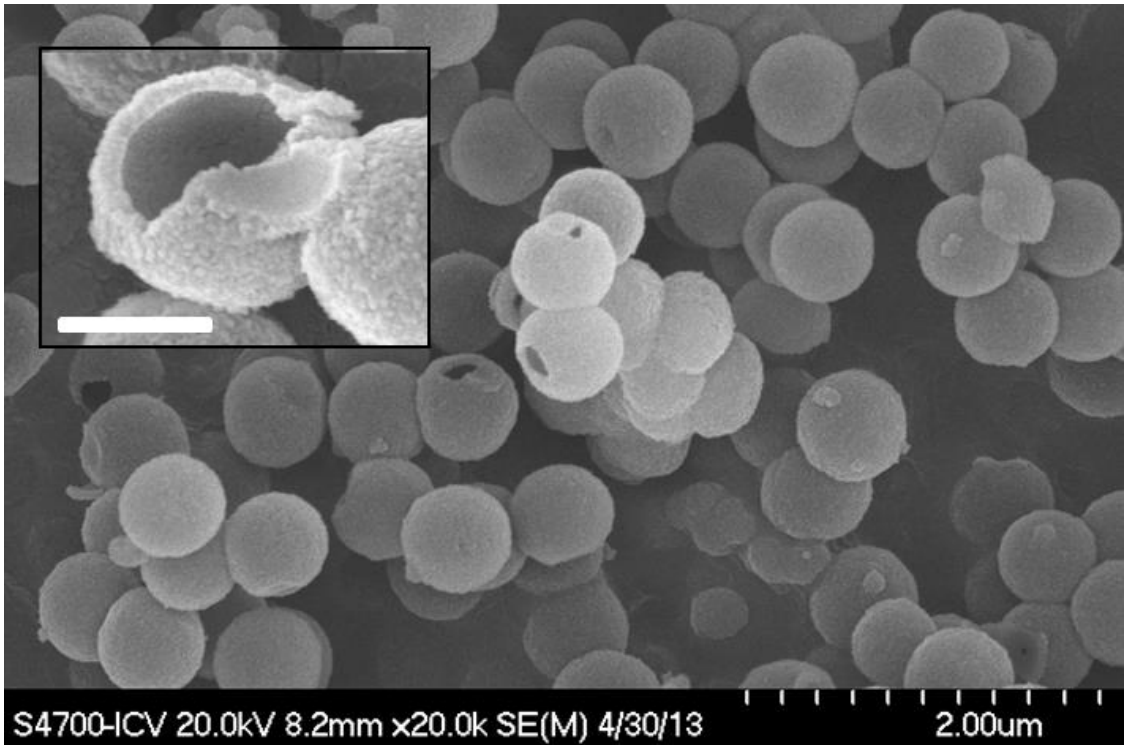

Figure 2. Scanning electron microscopic image representative of $@ZrO_2^{nc}$ particles showing holes that shows hollow cores. Inset: One magnified broken @shell particle that shows a hollow core and part of the ejected shell hanging on the right of the opening (scale bar 500 nm).

Fluoride removal from water solutions

Fluoride concentration decreased in solution with all four tested materials in less than 10 min. As a representative example, Figure 3 exposes the fluoride concentration in solution when contacted with $SiO_2@ZrO_2^{nc}$. In this experiment, fluoride concentration sharply decreased from 10 to 1.2 ppm in less than 10 min and remained constant after that (24 hr). The other three types of nanostructured colloids also exhibited similar behaviors with final concentrations below 1.1 ppm (see inset in Figure 3). Summing up, all synthesized colloidal particles rapidly decontaminated the water from its fluoride content, as the final concentration in water was below the ca. 2 ppm threshold recommended by the WHO [3].

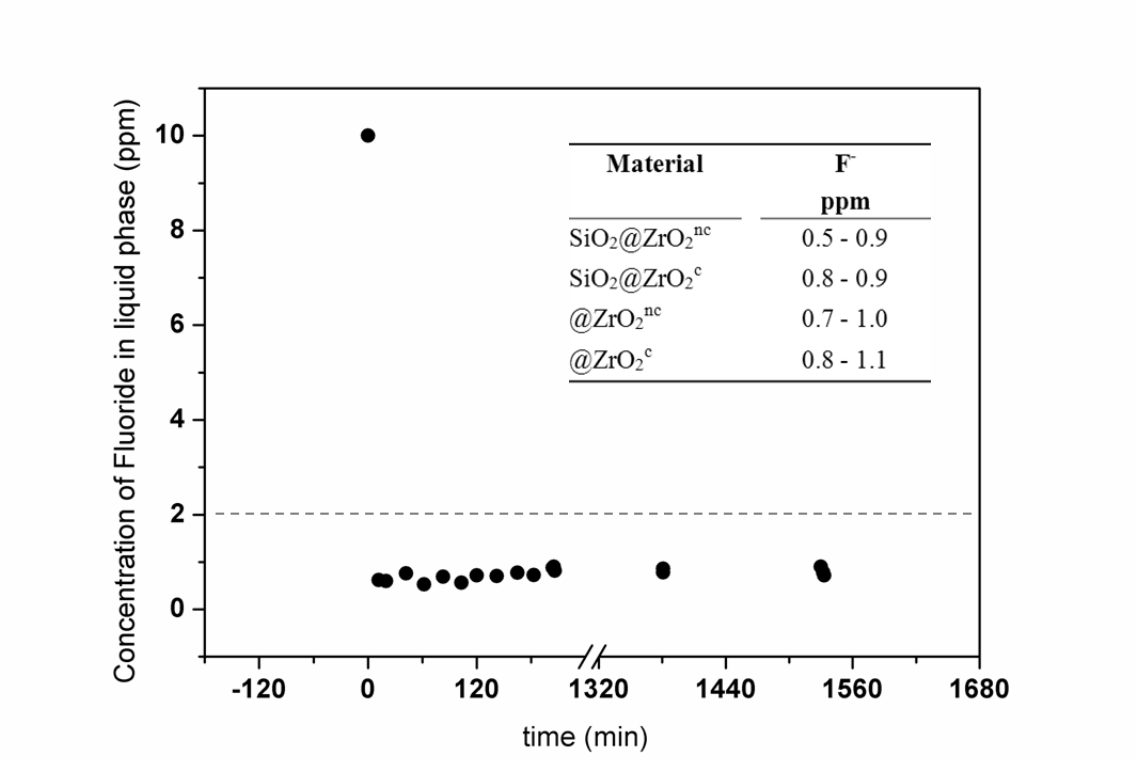

Figure 3. The concentration of fluoride (ppm) in the liquid phase from the batch system formed by $SiO_2@ZrO_2^{nc}$ and standard solution of fluoride (10 ppm) depicted as a function of time (min). Inset: $[F^-]$ in the liquid phase (right column) for the four types of materials (left column) at 24 h. The horizontal dashed line represents the maximum guideline value for fluoride in the water suggested by the World Health Organization.

Leaching of atoms from the solid into the solution followed by ICP-MS

A detailed study showed that time, pH and fluoride concentration (all variables from the batch mode experiment) influenced on the leaching of Na, Si, and Zr from the solid to the solution. The experimental design determined that the leaching process depended on time, pH, and fluoride concentration (*first-order coefficients*), those variables interacting with themselves (*quadratic coefficients*), and the interaction of two different variables (*cross-product coefficients*). Table 2 summarizes the information obtained from these experiments. Those variables that significantly influence (ANOVA, α = 0.05) the leaching of those elements carry a black dot.

Table 2. First-order coefficients, quadratic coefficients, and cross-product coefficients of the quadratic RSM model that showed a statistically significant influence (ANOVA, α = 0.05) present a star (*) in the table. The measured values of element concentration are available in Table S1 (supplementary information)

Solid	Elements in solution	First Order coefficients			Quadratic coefficients			Cross-product coefficients		
		t	pH	C	t*t	pH*pH	C*C	t*C	pH*C	t*pH
$SiO_2@ZrO_2^{nc}$	Na									
	Si	●			●	●				
	Zr	●			●			●		
$SiO_2@ZrO_2^{c}$	Na									
	Si	●	●							
	Zr	●	●	●		●				
$@ZrO_2^{nc}$	Na					●				●
	Si	●	●		●	●				●
	Zr									
$@ZrO_2^{c}$	Na				●					
	Si	●			●					●
	Zr	●	●	●	●					

Table 2 offers some crucial pieces of information. First, leaching of Si and Zr continued from the dispersed colloidal particles in most cases long after fluoride concentration equilibrated (*ca.* 10 min). Si and Zr concentrations significantly changed with time in most cases. Also, their dependence on quadratic coefficients and cross-product coefficients showed a more complicated dependence of leaching with experimental variables.

Second, core@shell particle, but not @shell particles, leached Na. Leaching of Na from @hollow particles did not significantly change with time (first-order coefficient). Still, it did significantly depend on the interaction of time with itself (quadratic coefficients) and with pH (cross-product coefficient). As hollow spheres formed by dissolving the silica core in

1N NaOH solution, the observed behavior suggests that some Na ions remained in hollow spheres despite the careful washing of the particles with distilled water.

Third, only particles with a crystalline shell showed a significant change in the amount of leached Zr with fluoride concentration. Leaching of Zr did not significantly change in particles with non-crystalline shells.

Leaching experiments showed that Si and Zr left the surface and diffused into the bulk solution (see concentrations in Table S1) long after fluoride concentration reached its equilibrium value. However, the chemical nature of the soluble species involving Si and Zr remained unclear. Those elements could have been aquo-complexes but also fluoro-complexes that formed after fluoride adsorption onto the surface.

Equation (2) proved that the amount of dissolved zirconium accounted for less than 1% of the fluoride removed from a solution in most cases (see Table 3). In only 4 out of 68 experiments, the concentration of dissolved Zr could explain between 2 and 7% of the fluoride removal process. Equation (2) assumes the formation of hexafluorocomplexes of Zr (ZrF_6^{2-}). If fluoride would react with zirconium to form soluble complexes with less than 6 fluorides per Zr atom, then the amount of fluoride removed from solution by formation of soluble fluorocomplexes would be even lower.

Table 3. The maximal amount of fluoride (in %) that disappeared from the solution that could be explained if ZrF_6^{2-} formed in a batch system for all four materials in all 17 experimental conditions tested for each material..

Sample	X =			
	SiO_2@ZrO_2^{nc}	**SiO_2@ZrO_2^{c}**	**@ZrO_2^{c}**	**@ZrO_2^{nc}**
X,1	1.49	0.10	0.56	0.61
X,2	0.28	0.08	0.16	0.15
X,3	3.11	0.03	0.62	0.61
X,4	0.49	0.03	0.17	0.15
X,5	0.35	0.02	0.24	0.20
X,6	0.60	0.02	0.21	0.25
X,7	0.43	0.02	0.25	0.24
X,8	1.46	0.02	0.56	0.76
X,9	0.24	0.01	0.17	0.19
X,10	0.58	0.01	0.23	0.21
X,11	0.54	0.01	0.25	0.28
X,12	0.25	0.01	0.25	0.33
X,13	3.62	0.03	0.41	1.15
X,14	3.73	0.02	0.12	0.22

X,15	6.88	0.01	0.50	0.51
X,16	6.33	0.01	0.14	0.17
X,17	2.17	0.01	0.20	0.22

Furthermore, equation (2) modified for Si proved that the amount of dissolved Si did neither satisfactorily explain the removal of fluoride from the solution as hexafluorocomplexes of silicon (SiF_6^{2-}). Under this assumption, the amount of Si in solution would explain only partial removal of fluoride in about half of the conditions tested, suggesting that a second removal mechanism would be necessary to explain the complete removal of fluoride (Table 4). In the other half of the conditions tested (Table 4), there was not enough fluoride to explain the total silicon concentration in the solution. Again, another leaching mechanism should occur to explain the total silicon concentration measured. Thus, it seems unlikely that the fluoride concentration in solution rapidly decreased because of the formation of soluble silicon fluorocomplexes.

Table 4. The maximal amount of fluoride (in %) that disappeared from the solution that could be explained if SiF_6^{2-} formed in a batch system for all four materials in all 17 experimental conditions tested for each material.

Sample	**X =**			
	$SiO_2@ZrO_2^{nc}$	**$SiO_2@ZrO_2^{c}$**	**$@ZrO_2^{c}$**	**$@ZrO_2^{nc}$**
X,1	121	27	331	253
X,2	24	5	69	51
X,3	128	27	344	253
X,4	26	6	70	51
X,5	56	9	115	84
X,6	65	9	119	101
X,7	61	10	121	96
X,8	142	28	369	284
X,9	29	6	72	57
X,10	47	9	119	97
X,11	47	9	119	96
X,12	46	10	119	95
X,13	167	29	375	338
X,14	37	6	73	65
X,15	160	30	356	301
X,16	35	6	72	61
X,17	51	9	118	99

So far, by studying fluoride removal kinetic and element leaching, we established a clearer picture of the process occurring as fluoride was removed using core@shell or @shell materials: fluoride ions diffused towards the material interface, were adsorbed, and reached equilibrium in less than 10 min, whereas element leaching continued long after fluoride concentrations had equilibrated.

FT-IR analyses were performed on the materials before and after been subjected to leaching. The obtained results suggest that fluoride bound to zirconium oxide displacing hydroxyl groups. For $@ZrO_2^{nc}$ and $@ZrO_2^{c}$, a band at 1360 cm^{-1} and a doublet at 1570 cm^{-1} are visible. Those bands are associated with bending vibration of Zr–OH groups and Zr–OH vibration, respectively. Both bands sharply decrease after the nanostructured particles were contacted with fluoride solution (Figure S4), confirming that fluoride replaced –OH groups [11], [15]. In the case of $SiO_2@ZrO_2^{nc}$ and $SiO_2@ZrO_2^{c}$, the exchange of hydroxyl group by fluoride ions could not be observed as for the proper bands (1000-1300 cm^{-1}).

Discussion and Conclusion

We found that all nanostructured spheres ($SiO_2@ZrO_2^{nc}$, $SiO_2@ZrO_2^{c}$, $@ZrO_2^{nc}$, and $@ZrO_2^{c}$) tested in our work reduced fluoride concentration from 10 ppm down to non-toxic values in less than 10 min. In all cases, fluoride bound to the solid particles without forming soluble fluorocomplexes. These results manifest that these four types of colloidal architectures with a shell of zirconium oxide are particularly interesting for fluoride removal.

The rapid extraction kinetics of the materials in this study (equilibration time <10 min) place these materials among the top materials currently known in fluoride removal. Among the materials reported in the literature, mesostructured zirconium phosphate was able to reduce 96% of the fluoride concentration (10 ppm) in *ca.* 15 min [16]. Carboxylated chitosan beads loaded with Zr were able to reach equilibrium in 40 min [5]. Iron(III)-zirconium(IV) hybrid oxide particles removed 90% of adsorbed fluoride (initial concentration range 5.0 – 25.0 ppm) in 45 min, though required more than 90 min to reach equilibrium [17]. Nanosized hydrous zirconium oxide within a polystyrene anion exchange resine exposed to fluoride solution (200 – 600 ppm) reached equilibrium within two hours [6]. Finally, granular zirconium-iron oxide in contact with fluoride solutions of

10 – 30 ppm equilibrated within 3 h, but then again, more than 10 h were required when the initial concentration was 50 – 100 ppm [7]. Interestingly, though, none of these studies considered leaching of elements nor formation of soluble fluorocomplexes as parameters in their investigations.

The materials tested in this study have some additional advantages regarding fluoride removal. First, they have a high specific surface area (ca. 160—300 $m^2.g^{-1}$), as already shown in previous works [8], [18]. Since fluoride removal is assumed to be a surface driven process, their higher specific surface areas are a welcome feature. Second, because of their size (ca. 500 nm), they can be more easily separated from water than zirconium oxide nanoparticles having a similar specific surface area. Third, colloidal particles with zirconium oxide are generally less toxic than nanometer-sized particles, as already highlighted in previous studies [18], [19]. Finally, the rapid fluoride removal process makes these nanostructured colloids outstanding candidates for experiments in continuous flow-through conditions.

We found that fluoride bound to zirconium oxide while a complex process occurred at the interface. Element leaching (Na, Si, and Zr) continued long after fluoride concentration stabilized in the batch systems. Though, leaching due to a chemical attack of fluoride that produces soluble fluorocomplexes of either Zr or Si seemed unlikely.

These findings support the image of a somewhat more complicated process taking place at the solid-liquid interface than usually assumed. While fluoride binds to zirconium after displacing hydroxyl groups, fluoride diffuses from the bulk of the solution towards the surface of the particles during the first 10 min until the fluoride concentration equilibrates. Besides, partial dissolution of the solid enables diffusion of Na, Si, and Zr away from the solid to the solution. Si and Zr diffuse away from the surface but not as fluorocomplexes.

This study tends to demonstrate a very critical point: when studying the performance of solid aiming at removing pollutants from water, scientists should consider element leaching. One reason is that elements may leach because of a chemical reaction occurring between the solid surface and the pollutant. Another reason is that elements going from the solid to the solution due to a partial dissolution may play a key role in removing a pollutant. Without this consideration, the whole picture that emerges in a study about the process at the interface may be quite different from what occurs during the pollutant removal process.

In summary, our findings show that a complex process occured at the interfaces during fluoride removal. Fluoride anions diffused towards the surface where they attached to Zr, reaching equilibrium in less than 10 min. Moreover, Na, Si, and Zr leached from the surface in a process that continued at least several hours. Besides, this study suggests that we should consider the leaching of elements when planning experiments aiming at studying the removal of pollutants from water, because leaching may trigger processes that interfere and compete with pollutant removal.

Author Contributions

Dr. Iván Maisuls performed investigation and writing – review and editing. Dr. Yolanda Castro and Prof. Dr. Alicia Duran performed investigation and writing – review and editing. Prof. Dr. Dominic Lariviere performed writing – review and editing. Prof. Dr. Pablo M. Arnal performed conceptualization, funding acquisition, and writing – Original Draft.

Acknowledgments

This study was partially supported by CONICET (PIP-2013-0105) and PICT-2014-2583, and by Comisión de Investigaciones Científicas de la Provincia de Buenos Aires (fellowship for undergraduate students for Iván Maisuls). Authors thank Dr. Pablo Lebed for performing leaching experiments.

Conflict of Interest Statement

On behalf of all authors, the corresponding author states that there is no conflict of interest.

Bibliography

[1] P. L. Smedley, H. B. Nicolli, D. M. J. Macdonald, A. J. Barros, and J. O. Tullio, "Hydrogeochemistry of arsenic and other inorganic constituents in groundwaters from La Pampa, Argentina," *Appl. Geochemistry*, vol. 17, pp. 259–284, 2002.

[2] M. G. García *et al.*, "Geochemistry and health aspects of F-rich mountanous streams and groundwaters from sierras Pampeanas de Cordoba, Argentina,"

Environ. Earth. Sci., vol. 65, no. 2, 2012.

[3] J. Chilton *et al.*, *Fluoride in Drinking-water*. On behalf of the World Health Organization by IWA Publishing, 2006.

[4] J. A. Blackwell and P. W. Carr, "Study of the fluoride adsorption characteristics of porous microparticulate zirconium oxide," *J. Chromatogr.*, vol. 549, no. 1–2, pp. 43–57, 1991.

[5] N. Viswanathan and S. Meenakshi, "Synthesis of Zr(IV) entrapped chitosan polymeric matrix for selective fluoride sorption," *Colloids Surfaces B Biointerfaces*, vol. 72, no. 1, pp. 88–93, 2009.

[6] B. Pan, J. Xu, B. Wu, Z. Li, and X. Liu, "Enhanced Removal of Fluoride by Polystyrene Anion Exchanger Supported Hydrous Zirconium Oxide Nanoparticles," *Environ. Sci. Technol.*, vol. 47, no. 16, pp. 9347–9354, 2013.

[7] X. Dou, Y. Zhang, H. Wang, T. Wang, and Y. Wang, "Performance of granular zirconium-iron oxide in the removal of fluoride from drinking water," *Water Res.*, vol. 45, no. 12, pp. 3571–3578, 2011.

[8] P. M. Arnal, C. Weidenthaler, and F. Schüth, "Highly monodisperse zirconia-coated silica spheres and zirconia/ silica hollow spheres with remarkable textural properties," *Chem. Mater.*, vol. 18, no. 11, pp. 2733–2739, 2006.

[9] P. A. Bazula, "Nanostructured Oxidic Materials: Properties and Application of Core@Shell Spheres and Hollow Particles," Ruhr Universitaet Bochum, Bochum, 2010.

[10] P. M. Arnal, "The synthesis of monodisperse colloidal core@shell spheres and hollow particles," Ruhr-Universität Bochum, Bochum, 2006.

[11] X. Dou, D. Mohan, C. U. Pittman, and S. Yang, "Remediating fluoride from water using hydrous zirconium oxide," *Chem. Eng. J.*, vol. 198–199, pp. 236–245, 2012.

[12] X. P. Liao and B. Shi, "Adsorption of fluoride on zirconium(IV)-impregnated collagen fiber," *Environ. Sci. Technol.*, vol. 39, no. 12, pp. 4628–4632, 2005.

[13] E. Bellack and P. J. Schouboe, "Rapid photometric determination of fluoride in water: Use of sodium 2-(p-sulfophenylazo)-1,8-dihydroxynaphthalene-3,6-disulfonate-zirconium lake," *Anal. Chem.*, vol. 30, no. 12, pp. 2032–2034, 1958.

[14] G. E. P. Box, J. S. Hunter, and W. G. Hunter, *Statistics for experimenters: design, innovation, and discovery*. Wiley-Interscience, 2005.

[15] M. TOULLEC, C. J. SIMMONS, and J. H. SIMMONS, "Infrared Spectroscopic Studies of the Hydrolysis Reaction During Leaching of Heavy-Metal Fluoride Glasses," *J. Am. Ceram. Soc.*, vol. 71, no. 4, pp. 219–224, Apr. 1988.

[16] S. K. Swain, T. Patnaik, V. K. Singh, U. Jha, R. K. Patel, and R. K. Dey, "Kinetics, equilibrium and thermodynamic aspects of removal of fluoride from

drinking water using meso-structured zirconium phosphate," *Chem. Eng. J.*, vol. 171, no. 3, pp. 1218–1226, 2011.

[17] K. Biswas, K. Gupta, A. Goswami, and U. C. Ghosh, "Fluoride removal efficiency from aqueous solution by synthetic iron(III)-aluminum(III)-chromium(III) ternary mixed oxide," *Desalination*, vol. 255, no. 1–3, pp. 44–51, 2010.

[18] A. L. Di Virgilio, P. M. Arnal, and I. Maisuls, "Biocompatibility of core at shell particles: Cytotoxicity and genotoxicity in human osteosarcoma cells of colloidal silica spheres coated with crystalline or amorphous zirconia," *Mutat. Res. - Genet. Toxicol. Environ. Mutagen.*, vol. 770, pp. 85–94, 2014.

[19] A. L. A. L. Di Virgilio, I. Maisuls, F. Kleitz, and P. M. Arnal, "A new synthesis pathway for colloidal silica spheres coated with crystalline titanium oxide and its comparative cyto- and genotoxic study with titanium oxide nanoparticles in rat osteosarcoma (UMR106) cells," *J. Colloid Interface Sci.*, vol. 394, no. 1, pp. 147–156, 2013.

Rapid removal of fluoride from water using core@shell and @shell nanoparticles of SiO_2@ZrO_2 and @ZrO_2. Investigation of the mechanisms involved and impact of elemental leaching

Supplementary Information

Deduction of equation (10)

$$\frac{mol_F}{mol_{Zr}} = \frac{\frac{m_F}{AW_F}}{\frac{m_{Zr}}{AW_{Zr}}} \quad (3)$$

$$(\dots) = \frac{\frac{ppm_F . V_{sc}}{AW_F}}{\frac{ppm_{Zr} . V_{sc}}{AW_{Zr}}} \quad (4)$$

$$(\dots) = \frac{\frac{ppm_F}{AW_F}}{\frac{ppm_{Zr}}{AW_{Zr}}} \quad (5)$$

$$(\dots) = \frac{ppm_F \,.\, AW_{Zr}}{ppm_{Zr} \,.\, AW_F} \quad (6)$$

$$\%F = 100 \,.\frac{mol\ F\ in\ ZrF_6^{2-}}{mol\ F} \tag{7}$$

$$\%F = 100 \,.\, 6 \,.\frac{mol\ Zr}{mol\ F} \tag{8}$$

Introducing (6) in (8) yields

$$\%F = 600 \,.\frac{ppm_{Zr}\,.\,AW_F}{ppm_F\,.\,AW_{Zr}} \tag{9}$$

Where (9) is shown above.

Replacing ppm_{Zr} and ppm_F by [Zr] and [F-] in (9) yields:

$$\%F = 600 \,.\frac{[\boldsymbol{Zr}]\,.\,AW_F}{[F^-]\,.\,AW_{Zr}} \tag{10}$$

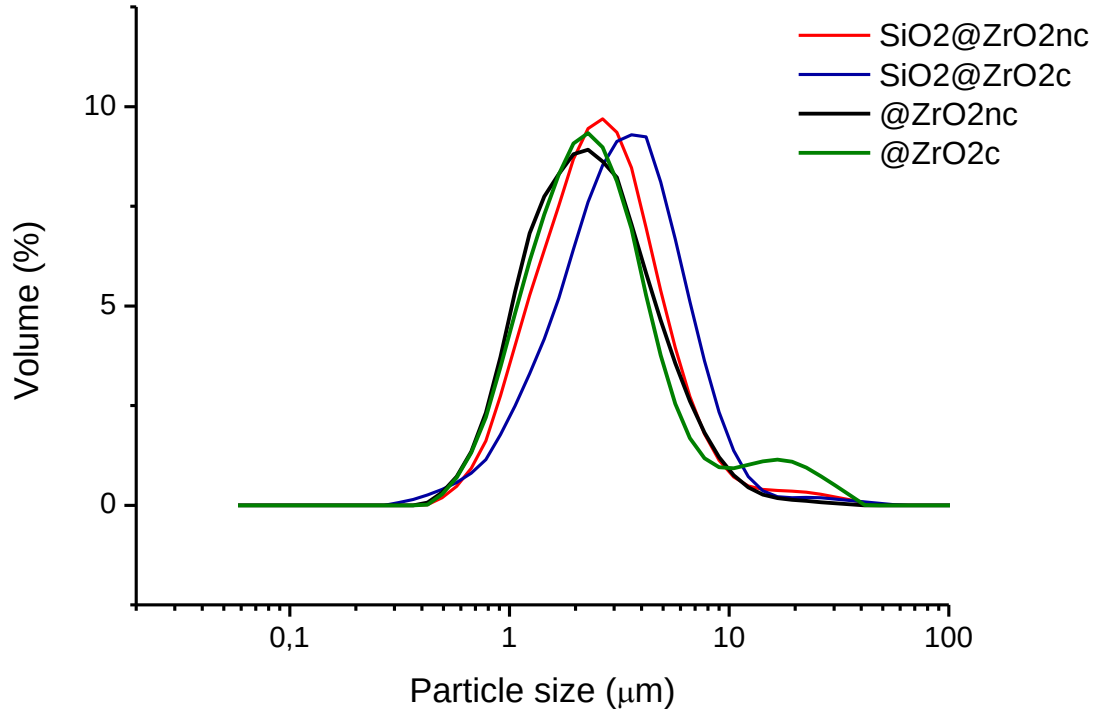

Figure S1. The size distribution of solid core@shell and @shell particles in dilute dispersions.

Table S1. The concentration of elements Na, Si and Zr (ppm) in the liquid phase measured with ICP-MS for each of the four types of material in the 17 different experiments performed in each face-centered central composite experimental

Code	$SiO_2@ZrO_2^{nc}$			$SiO_2@ZrO_2^{c}$			$@ZrO_2^{nc}$			$@ZrO_2^{c}$		
	Na ppm	Si ppm	Zr ppm	Na ppm	Si ppm	Zr ppm	Na ppm	Si ppm	Zr ppm	Na ppm	Si ppm	Zr ppm
1	0.030	0.665	0.027	0.025	0.146	0.002	2.729	1.392	0.011	2.619	1.819	0.010
2	0.055	0.672	0.025	0.021	0.148	0.007	2.784	1.389	0.013	2.716	1.892	0.014
3	0.019	0.700	0.056	0.007	0.148	0.001	2.764	1.388	0.011	2.656	1.891	0.011
4	0.036	0.707	0.045	0.033	0.152	0.003	2.769	1.403	0.013	2.729	1.917	0.015
5	0.033	0.919	0.019	0.016	0.149	0.001	2.763	1.378	0.011	2.675	1.887	0.013
6	0.057	1.074	0.032	0.015	0.148	0.001	2.849	1.669	0.014	2.702	1.957	0.011
7	0.032	1.009	0.023	0.019	0.167	0.001	2.797	1.587	0.013	2.754	1.987	0.013
8	0.032	0.779	0.026	0.027	0.152	0.000	2.780	1.558	0.014	2.828	2.024	0.010
9	0.029	0.783	0.022	0.025	0.157	0.001	2.769	1.572	0.017	2.758	1.973	0.015
10	0.018	0.774	0.032	0.014	0.150	0.001	2.778	1.603	0.011	2.724	1.962	0.012
11	0.019	0.780	0.029	0.077	0.152	0.001	2.765	1.576	0.015	2.725	1.966	0.013
12	0.030	0.765	0.014	0.031	0.157	0.001	2.775	1.557	0.018	2.748	1.953	0.014
13	0.055	0.919	0.065	0.025	0.156	0.001	2.863	1.855	0.021	2.727	2.057	0.007
14	0.033	1.006	0.337	0.025	0.153	0.001	2.828	1.772	0.020	2.675	2.014	0.011
15	0.016	0.880	0.124	0.011	0.167	0.000	2.711	1.651	0.009	2.612	1.956	0.009
16	0.040	0.968	0.571	0.037	0.159	0.001	2.780	1.677	0.015	2.625	1.964	0.013
17	0.055	0.833	0.117	0.028	0.155	0.000	2.699	1.633	0.012	2.603	1.941	0.011

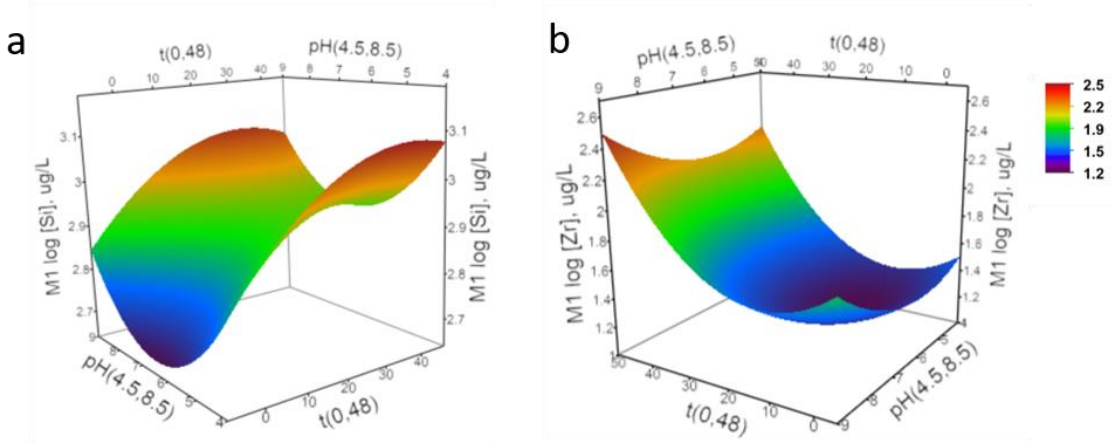

Figure S2. Modeled response surface plot showing the log concentration of leached a) Si and b) Zr as a function of pH and time.

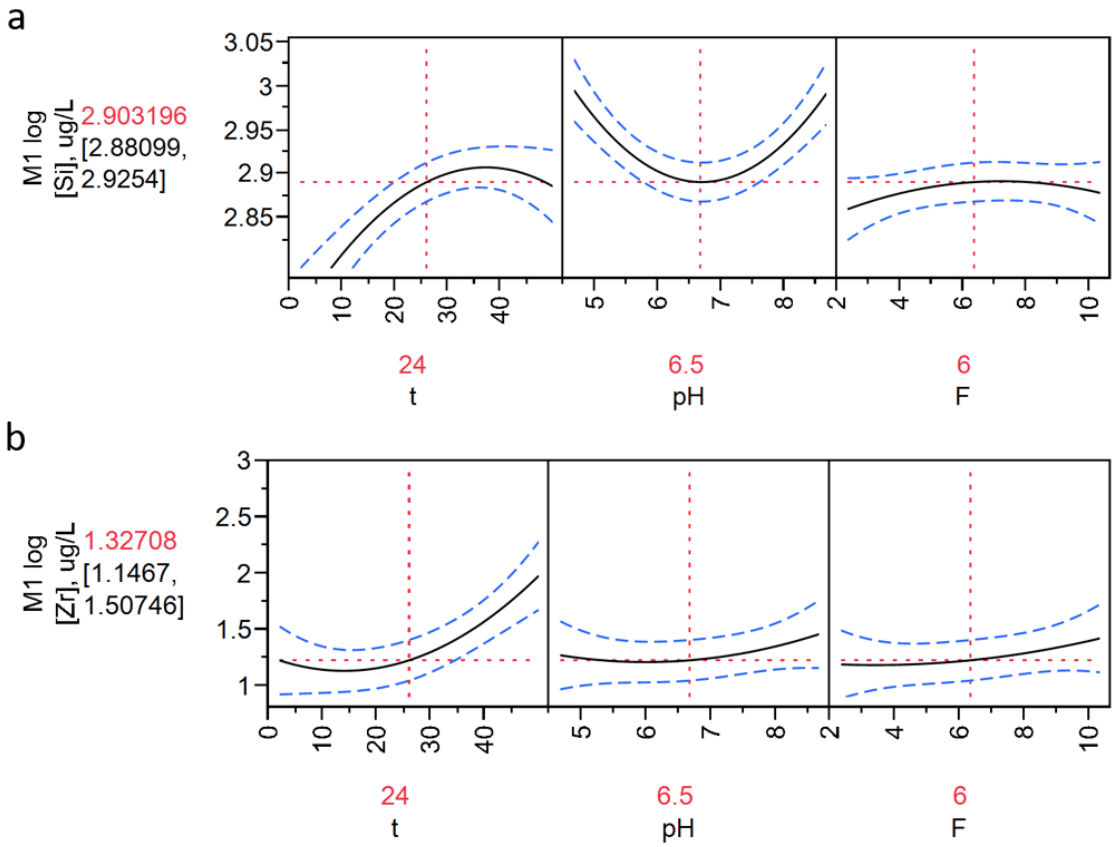

Figure S3. Predicted individual response plots showing the log concentration of leached a) Si and b) Zr as a function of pH and time. To calculate an individual response the remaining variables were fixed to t= 24, pH = 6.5 and [F] = 6 ppm.

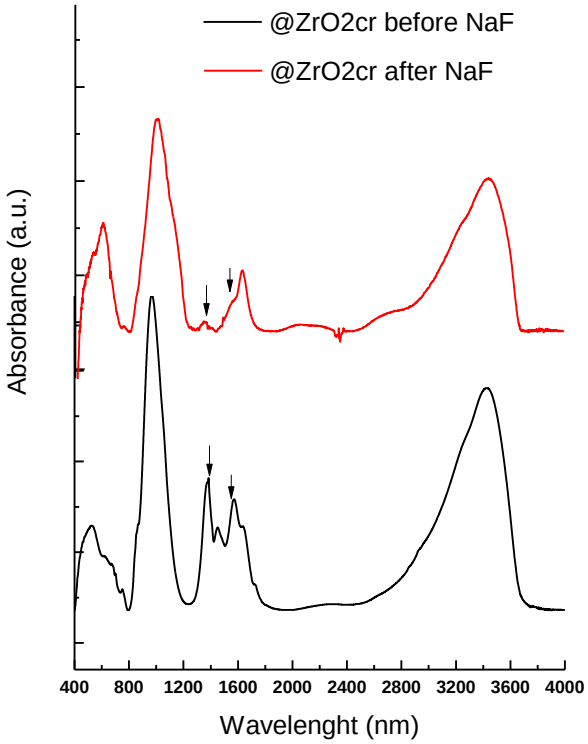

Figure S4. FTIR spectra of @ZrO_2c before and after fluoride absorption.